Effect of Saturation of Polydienes with Varying Microstructures on the Phase Behavior of Poly(vinylcyclohexane)/Poly(ethylene-*alt*-propylene) and Poly(vinylcyclohexane)/Poly(ethylene-*co*-1-butene) Blends

Chang Dae Han,* Kyung Min Lee, and Soobum Choi

Department of Polymer Engineering, The University of Akron, Akron, Ohio 44325

Stephen F. Hahn

Central Research and Development, The Dow Chemical Company, Midland, Michigan 48674

Received May 28, 2002

ABSTRACT: The effect of saturation of polydienes with varying microstructures on the phase behavior of poly(vinylcyclohexane) (PVCH)/poly(ethylene-*co*-1-butene) (PEB) and PVCH/poly(ethylene-*alt*-propylene) (PEP) blends was investigated. For the study, a series of polyisoprenes (PI) and polybutadienes (PB) with varying microstructures and molecular weights and polystyrenes (PS) with varying molecular weights were synthesized via anionic polymerization. Subsequently, they were saturated, yielding PVCH, PEB, and PEP, respectively. Binary blends of PVCH and PEB and binary blends of PVCH and PEP with blend compositions varying from 10 to 90 wt % were prepared from solvent casting in toluene. Laser light scattering was used to take cloud point measurements, which were then used to construct phase diagrams. For comparison, the phase behavior of PS/PI and PS/PB blends was also investigated. It was found that the PVCH/PEB and PVCH/PEP blends exhibit upper critical solution temperature, similar to the PS/PI and PS/PB blends. The interaction parameter for each polymer pair chosen was determined by curve-fitting the experimental phase diagram to a theoretical phase diagram predicted from the Flory−Huggins theory. The interaction parameters thus obtained were used to predict, via the currently held mean-field theory, the order−disorder transition temperature (T_{ODT}) of the PVCH-*block*-PEB and PVCH-*block*-PEP copolymers reported in the literature. It has been found that the predicted T_{ODT} of the PVCH-*block*-PEP and PVCH-*block*-PEB copolymers is higher than that of the unsaturated precursors having PI or PB blocks with predominantly 1,4-addition. These findings are in agreement with the experimental results reported in the literature. It is concluded that the experimentally observed increase in T_{ODT} after complete saturation of SI or SB diblock copolymers having PI or PB blocks with predominantly 1,4-addition is due to the substantial increase in the repulsive segment−segment interactions between PVCH and PEP and between PVCH and PEB.

1. Introduction

For the past four decades, diene-based block copolymers, such as polystyrene-*block*-polyisoprene (SI diblock), polystyrene-*block*-polybutadiene (SB diblock), polystyrene-*block*-polyisoprene-*block*-polystyrene (SIS triblock), and polystyrene-*block*-polybutadiene-*block*-polystyrene (SBS triblock), have enjoyed commercial success. However, these block copolymers suffer from the thermal instability in that the polydiene block, particularly the polybutadiene (PB) block, readily undergoes thermal degradation/cross-linking reactions at elevated temperature (roughly 180 °C). This problem can be alleviated by selectively saturating the polydiene block.

For example, a polydiene-saturated triblock copolymer with the structure polystyrene-*block*-poly(ethylene-*co*-1-butene)-*block*-polystyrene (SEBS triblock) has been commercialized (e.g., Kraton G Series, Kraton Polymers) and is prepared by selectively saturating the PB midblock of an SBS triblock copolymer. The PB block in all commercial SB diblock or SBS triblock copolymers has microstructures consisting of 1,4-addition and 1,2-addition. The saturation of PB yields polymers that are structurally identical with poly(ethylene-*co*-1-butene) (PEB) consisting of ethylene units (which come from the saturation of 1,4-addition) and 1-butene units (which come from the saturation of 1,2-addition). As expected, SEBS triblock copolymer is much more thermally stable than the unsaturated precursor.

However, from a processing point of view, SEBS triblock copolymer suffers from a very high melt viscosity, because microdomain structures in the SEBS triblock copolymer persist at usual processing temperatures (up to about 260 °C). The melt viscosity of a block copolymer in the ordered (microphase-separated) state is much higher (a few orders of magnitude) than that in the disordered (homogeneous) state.[1,2] This means that from a processing point of view it is highly desirable to keep the order−disorder transition temperature (T_{ODT}) of a block copolymer below the processing temperature to control the melt viscosity of a block copolymer. In fact, the T_{ODT} of commercially available SEBS triblock copolymers is much higher than 300 °C,[3] which arises from the fact that the repulsive segment−segment interaction between polystyrene (PS) and PEB are much stronger than that between PS and PB.

Today it is well established, theoretically[4,5] and experimentally,[6,7] that the T_{ODT} of a block copolymer depends on the molecular weight, block copolymer composition, and the extent of repulsive segment−segment interactions (for simplicity, hereafter this will be referred to as the interaction parameter) between the constituent blocks. There are two ways of lowering the T_{ODT} of a block copolymer: one is to decrease the molecular weight, and the other is to make the segment−segment interactions between the constituent components *less* repulsive. Decreasing the molecular

10.1021/ma0208178 CCC: $22.00
Published on Web 09/06/2002

weight of a block copolymer, however, will sacrifice the mechanical properties. Then, the only alternative left to us is to modify the chemical structure of a block copolymer, such that the chemical modification can achieve two objectives at the same time: (i) an increase in thermal stability and (ii) a decrease in T_{ODT}. This can be achieved when the repulsive segment−segment interactions between the constituent blocks are reduced (i.e., when the miscibility of two chemically dissimilar blocks is improved). One such approach might be to saturate, for instance, both the PS and polydiene blocks of SB, SI, SBS, or SIS block copolymers. Indeed, some attempts toward that direction have been reported.[8−12] Specifically, both blocks in an SB diblock copolymer were saturated to obtain poly(vinylcyclohexane) (PVCH)-*block*-PEB copolymer, and both blocks in SI diblock copolymer were saturated to obtain PVCH-*block*-poly(ethylene-*alt*-propylene) (PEP) copolymer. It has been reported that the glass transition temperature (T_g) of PVCH is much higher (ca. 40 °C) than that of PS.[13] Thus, PVCH-*block*-PEB and PVCH-*block*-PEP copolymers offer opportunities for high-temperature applications. Polyisoprene (PI) having predominantly 1,4-addition (greater than 90%) can be obtained when isoprene is polymerized in cyclohexane as solvent, or PI having high vinyl content (i.e., predominantly 3,4- and 1,2-additions) can be obtained when isoprene is polymerized in tetrahydrofuran as solvent. Saturation of PI yields poly(ethylene-*alt*-propylene) (PEP).

According to the recent literature,[8−11] the T_{ODT} of PVCH-*block*-PEP copolymers was found to be 7−32 °C higher than that of the unsaturated precursor having a PI block with predominantly 1,4-addition, suggesting that the segment−segment interactions between PVCH and PEP became *more repulsive* after the saturation of PS and PI blocks. This trend was found to be the opposite of that predicted from calculations, via group contribution methods, of the interaction parameters for PVCH/PEP and PS/PI pairs.[8−10] If the predictions based on group contribution methods were accurate, the T_{ODT} of a PVCH-*block*-PEP copolymer should be lower than that of the unsaturated precursor. Having found that the interaction parameters for the PVCH/PEP and PS/PI pairs calculated from group contribution methods could not explain their experimental results, Gehlsen and Bates[8] concluded that the experimentally observed increase in T_{ODT} of a PVCH-*block*-PEP copolymer was due to an increase in conformational asymmetry after the saturation of SI diblock copolymer. Interestingly, Adams et al.[10] reported an increase in T_{ODT} of a PVCH-*block*-PEB copolymer by as much as 124 °C over that of the unsaturated precursor having a PB block with predominantly 1,4-addition. However, Gehlsen and Bates[9] reported that the T_{ODT} of a PVCH-*block*-PEB copolymer was much lower than that of the unsaturated precursor having a PB block with predominantly 1,2-addition.

The present study was motivated by the need to explain the experimental results of T_{ODT} measurements of PVCH-*block*-PEB and PVCH-*block*-PEP copolymers reported in the literature[8−11] by investigating the phase behavior of PVCH/PEB, PS/PB, PVCH/PEP, and PS/PI pairs from cloud point measurements. For the investigation, we synthesized, via anionic polymerization, a series of PBs and PIs with varying microstructures and molecular weights, and PSs with varying molecular weights, and then saturated each of them to obtain PEB, PEP, and PVCH, respectively. Then we prepared PS/PI, PVCH/PI, PS/PEP, PVCH/PEP, PS/PB, PVCH/PB, PS/PEB, and PVCH/PEB binary blends to measure cloud points using laser light scattering and to construct phase diagrams. The phase diagrams thus constructed enabled us to explain satisfactorily the experimental results of T_{ODT} measurements of PVCH-*block*-PEP and PVCH-*block*-PEB copolymers reported in the literature.[8−11] We have found that group contribution methods are not sensitive enough to discern the differences in the microstructures of a polydiene mixed with PS or PVCH. Experimental phase diagrams were curve-fitted to theoretically predicted ones from the Flory−Huggins theory to obtain an expression for the temperature-dependent interaction parameter. Using currently held mean-field theory together with the experimentally determined segment−segment interaction parameters obtained using binary blends, we were able to predict the T_{ODT}'s of the PVCH-*block*-PEP and PVCH-*block*-PEB copolymers reported in the literature.[8−11] We have found that the predicted T_{ODT}'s show the same trend as those observed experimentally. In this paper we report the highlights of our findings.

2. Experimental Section

Materials and Characterization. In this study we synthesized, via anionic polymerization, PSs with varying molecular weights and PIs with varying molecular weights and microstructures using standard procedures. PI having predominantly 1,4-addition was synthesized in cyclohexane as solvent, and PI having high vinyl content (i.e., predominantly 3,4- and 1,2-additions) was synthesized in tetrahydrofuran as solvent. In both cases, *sec*-butyllithium was used as initiator. We used PBs and PEBs with varying molecular weights and microstructures that were synthesized in our previous study,[14] in which the experimental procedures employed for the synthesis of the PBs and the saturation of the PBs to obtain PEBs are described in detail.

The PSs and PIs synthesized were saturated with hydrogen. Hydrogenation reactions were performed using cyclohexane (Fisher Scientific, HPLC grade) that was purified by passing over a column of activated alumina prior to use. A heterogeneous Pt/SiO_2 catalyst was used in all hydrogenations,[15] which were performed in a 2 L stainless steel pressure reactor (Parr Instrument) equipped with a gas dispersion impeller. The reactor was cleaned before use by heating 1.5 L toluene to 100 °C in the reactor under nitrogen, draining the hot toluene while still hot, evacuating and refilling with nitrogen, and allowing the reactor to cool to room temperature. Hydrogen (Scott Specialty Gases, 99.999%) was used without further purification. Gel permeation chromatography (GPC) was performed using an Agilent 1100 high performance liquid chromatograph equipped with two Polymer Labs PLGel Mixed C columns, using tetrahydrofuran as eluent at a flow rate of 1 mL/min at 40 °C and an injection volume of 50 μL. Output was detected using a differential refractometer detector, and the columns were calibrated using narrow polydispersity polystyrene standards (Polymer Laboratories). ^{1}H nuclear magnetic resonance (NMR) spectra were recorded on polymer samples dissolved in deuteriochloroform (0.05 g of polymer in 1.0 mL of $CDCl_3$) using a Varian INOVA 300 spectrometer. Specifically, polystyrene was hydrogenated using the following procedures.[15] First, 5 g of polystyrene was dissolved in 800 mL of cyclohexane and was then added to the reactor. A slurry containing 5 g of Pt/SiO_2 catalyst[16] in 200 mL of cyclohexane was prepared in a stainless steel cylinder equipped with air-free quick disconnecting fittings, and the slurry was transferred to the reactor with a slight overpressure of nitrogen. The reactor was purged twice with hydrogen, and the hydrogen pressure was set at 8.96 MPa (1300 psig). The reactor was then sealed and heated to 170 °C with stirring, and the reaction was allowed to proceed for 3 h. After this time the

Table 1. Summary of the Molecular Characteristics of the Homopolymers Employed for Cloud Point Measurements

sample code	M_n (g/mol)	M_w/M_n[a]	microstructure
PS-2	2200[b]	1.05	NA
PS-3	3100[b]	1.05	NA
PS-6	6000[b]	1.06	NA
PS-10	9500[b]	1.09	NA
PVCH-2	2327[c]		NA
PVCH-3	3268[c]		NA
PVCH-6	6346[c]		NA
PVCH-10	10577[c]		NA
$PI^{1,4}$-5	5000[b]	1.02	94% 1,4-addition
$PI^{3,4}$-6	6100[b]	1.09	high vinyl content[d]
$PI^{1,4}$-10	10000[b]	1.04	94% 1,4-addition
$PEP^{1,4}$-5	5150[c]		ethylene-*alt*-propylene
$PEP^{3,4}$-6	6280[c]		ethylene-*alt*-propylene
$PEP^{1,4}$-10	10300[c]		ethylene-*alt*-propylene
$PB^{1,4}$-26H[e]	3481[f]	1.05	26% 1,2 addition
$PB^{1,2}$-84H[e]	3629[f]	1.03	84% 1,2-addition
$PEB^{1,4}$-26H[e]	3610[f]	1.06	26% 1-butene
$PEB^{1,2}$-50H[e]	3720[f]	1.06	50% 1-butene
$PEB^{1,2}$-84H[e]	3877[f]	1.05	84% 1-butene

[a] Determined using gel permeation chromatography. [b] Determined using vapor pressure osmometry. [c] Calculated from stoichiometry. [d] 59% 3,4-addition and 34% 1,2-addition. [e] From ref 14. [f] Determined using mass spectrometry and thus the accuracy is good to the last digit.

reactor was allowed to cool to room temperature, and the excess hydrogen was vented. The polymer solution was separated from the catalyst using a 0.2 μm Teflon membrane filter, and the polymer was isolated by precipitation from methanol. After drying in a vacuum oven to remove residual solvent, the isolated polymer weighed 4.3 g. ^{1}H NMR analysis showed no detectable resonances due to the polystyrene phenyl ring, only a broad resonance ranging from 0.6 to 1.8 ppm. Similar procedures were used to hydrogenate polyisoprene. ^{1}H NMR analysis showed no detectable resonances due to the polyisoprene backbone alkenes in the starting material, only a sharp resonance due to the methyl group at 0.85 ppm and a broad resonance ranging from 1 to 1.8 ppm.

The number-average molecular weight (M_n) of all PSs and PIs synthesized in this study was determined using vapor pressure osmometry (Knauer), and the polydispersity index (M_w/M_n) of the polymers was determined using gel permeation chromatography (GPC) (Waters). Comparison of the GPC chromatogram before and after the saturation of PI showed little change in polydispersity index. The microstructures of the PIs synthesized in this study were determined using ^{1}H and ^{13}C NMR spectroscopy, and the microstructures of the PBs and PEBs employed in this study were determined in our previous study.[14] Table 1 gives a summary of the molecular characteristics of the polymers employed in this study and also the microstructures of PI, PEP, PB, and PEB. The values of M_n and M_w/M_n of the PBs and PEBs given in Table 1 were determined in our previous study.[14] The molecular weights of the saturated polymers given in Table 1 were calculated from stoichiometry. For convenience, as given in Table 1, throughout this paper we use the following notations: $PI^{1,4}$ and $PB^{1,4}$ describing the polydienes having predominantly 1,4-addition; $PEP^{1,4}$ and $PEB^{1,4}$ describing the saturated polymers from the unsaturated precursors $PI^{1,4}$ and $PB^{1,4}$, respectively; $PI^{3,4}$ and $PB^{1,2}$ describing the polydienes having predominantly 3,4-addition and 1,2-addition, respectively; $PEP^{3,4}$ and $PEB^{1,2}$ describing the saturated polymers from the unsaturated precursors $PI^{3,4}$ and $PB^{1,2}$, respectively.

Sample Preparation. Each of the PBs, PEBs, PIs, and PEPs was mixed with PVCH in toluene (ca. 10% solution) by varying the weight fraction of PVCH from 0.1 to 0.9 in the binary mixture, and subsequently a few drops of the solution were placed on a glass slide for cloud point measurements. The solvent was evaporated very slowly first at room temperature in a fume hood and then in a vacuum oven at an elevated temperature. Table 2 gives a summary of sample codes and the polymer pairs employed for cloud point measurements.

Table 2. Summary of Polymer Pairs Employed for Cloud Point Measurements

sample code	polymer pairs
	(a) PS/$PI^{1,4}$ and PVCH/$PEP^{1,4}$ Blends
PS/$PI^{1,4}$	(PS-2)/($PI^{1,4}$-5); (PS-3)/($PI^{1,4}$-5); (PS-6)/($PI^{1,4}$-5); (PS-6)/($PI^{1,4}$-10); (PS-10)/($PI^{1,4}$-5)
PS/$PEP^{1,4}$	(PS-2)/($PEP^{1,4}$-5); (PS-6)/($PEP^{1,4}$-5)
PVCH/$PI^{1,4}$	(PVCH-2)/($PI^{1,4}$-5); (PVCH-6)/($PI^{1,4}$-5)
PVCH/$PEP^{1,4}$	(PVCH-2)/($PEP^{1,4}$-5); (PVCH-6)/($PEP^{1,4}$-5); (PVCH-6)/($PEP^{1,4}$-10)
	(b) PS/$PI^{3,4}$ and PVCH/$PEP^{3,4}$ Blends
PS/$PI^{3,4}$	(PS-2)/($PI^{3,4}$-6)
PS/$PEP^{3,4}$	(PS-2)/($PEP^{3,4}$-6)
PVCH/$PI^{3,4}$	(PVCH-10)/($PI^{3,4}$-6)
PVCH/$PEP^{3,4}$	(PVCH-10)/($PEP^{3,4}$-6)
	(c) PS/$PB^{1,4}$ and PVCH/$PEB^{1,4}$ Blends
PS/$PB^{1,4}$	(PS-2)/($PB^{1,4}$-26H)
PS/$PEB^{1,4}$	(PS-2)/($PEB^{1,4}$-26H)
PVCH/$PB^{1,4}$	(PVCH-2)/($PB^{1,4}$-26H)
PVCH/$PEB^{1,4}$	(PVCH-2)/($PEB^{1,4}$-26H)
	(d) PS/$PB^{1,2}$ and PVCH/$PEB^{1,2}$ Blends
PS/$PB^{1,2}$	(PS-2)/($PB^{1,2}$-84H)
PS/$PEB^{1,2}$	(PS-2)/($PEB^{1,2}$-84H)
PVCH/$PB^{1,2}$	(PVCH-2)/($PB^{1,2}$-84H)
PVCH/$PEB^{1,2}$	(PVCH-2)/($PEB^{1,2}$-84H); (PVCH-3)/($PEB^{1,2}$- 84H); (PVCH-6)/($PEB^{1,2}$-84H); (PVCH-10)/($PEB^{1,2}$-84H); (PVCH-10)/($PEB^{1,2}$-50H); (PVCH-10)/($PEB^{1,2}$-26H)

Cloud Point Measurement. The cloud point of a specimen was determined using laser light scattering. Specifically, a glass slide containing a specimen was placed on the hot stage of the sample holder attached with a programmable temperature controller. A low-power He−Ne laser (wavelength of 635 nm) was used as the light source, and a photodiode was used as the detector.

A specimen was first heated to a temperature slightly (ca. 20 °C) above the cloud point (i.e., in the isotropic region) followed by a slow cooling into the two-phase region where a change in light intensity was noticeable, and then the specimen was heated again at a preset rate (0.5−5 °C/min), during which information on both temperature and the intensity of scattered light was stored on a diskette. For each composition of a particular blend system, cloud point measurements were repeated 3−5 times until data were reproducible, and a fresh specimen was used for each experimental run. For a given blend system, 8−9 compositions from 10/90 to 90/10 blend ratios were used to measure cloud point. A plot of the intensity of scattered light vs temperature during heating was prepared, which then allowed us to construct a phase diagram, the results of which will be presented below. We had to conduct a preliminary experiment for each polymer pair to determine an optimum range of the molecular weight. When taking cloud points for a polymer pair containing PB or PI, we chose the molecular weight, such that the maximum (critical) temperature of the pair did not exceed 190 °C to avoid significant thermal degradation and/or cross-linking reactions.

3. Results and Discussion

Below we will first present phase diagrams for each blend system investigated, placing emphasis on the role that the saturation of polydiene has played in determining the phase behavior of PVCH/PEP and PVCH/PEB pairs. Then we will determine expressions for segment−segment interaction parameters of PS/$PI^{1,4}$, PVCH/$PEP^{1,4}$, PS/$PI^{3,4}$, PVCH/$PEP^{3,4}$, PS/$PB^{1,4}$, PVCH/$PEB^{1,4}$, PS/$PB^{1,2}$, and PVCH/$PEB^{1,2}$ pairs by curve-fitting the experimental phase diagram to the theoretical phase diagram predicted from the Flory−Huggins theory. Using the segment−segment interaction parameters thus determined, we will predict, via mean-field theory, the T_{ODT}'s of the PVCH-*block*-$PEP^{1,4}$ and PVCH-*block*-

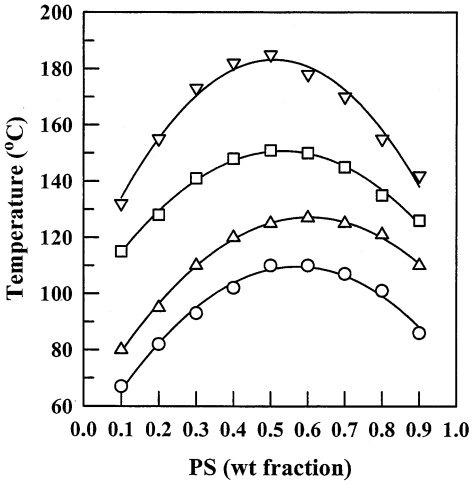

Figure 1. Phase diagrams for (○) (PS-2)/(PI^{1,4}-5) blends with T_c = 110 °C, (△) (PS-3)/(PI^{1,4}-5) blends with T_c = 125 °C, (□) (PS-6)/(PI^{1,4}-5) blends with T_c = 151 °C, and (▽) (PS-10)/ (PI^{1,4}-5) blends with T_c = 185 °C.

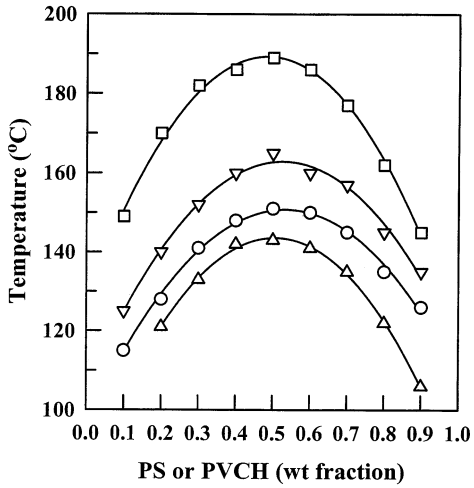

Figure 2. Phase diagrams for (○) (PS-6)/(PI^{1,4}-5) blends with T_c = 151 °C, (△) (PVCH-6)/(PI^{1,4}-5) blends with T_c = 143 °C, (□) (PS-6)/(PEP^{1,4}-5) blends with T_c = 189 °C, and (▽) (PVCH-6)/(PEP^{1,4}-5) blends with T_c = 165 °C.

PEB^{1,4} copolymers reported by previous investigators and compare with experimental results.[8−11]

Phase Diagrams of PS/PI^{1,4} and PVCH/PEP^{1,4} Blends. Figure 1 gives phase diagrams of four pairs of PS and PI, in which only the molecular weight (M_n) of PS is increased by keeping the same PI (PI^{1,4}-5) (see Table 1). It is clearly seen that the binodal curve is shifted upward; the critical temperature (T_c) is increased from 110 to 185 °C as the M_n of PS is increased from 2200 to 9500 g/mol. This means that predicted values of T_{ODT} using mean-field theory will be different, depending on which of the binodal curves given in Figure 1 is used to obtain an expression for segment−segment interaction parameter, which will be discussed later in this paper. This observation suggests that one must use the same molecular weight (more precisely speaking, the same number of repeat units, polymerization index N) to obtain cloud points (thus segment−segment interaction parameter) for all polymer pairs and their saturated counterparts. This should minimize (if not eliminate completely) the effect of molecular weight on cloud points (i.e., blend miscibility).

Otherwise, a comparison of predicted T_{ODT} of SI or SB diblock copolymer with that of the saturated counterparts is not warranted. As will be shown below, in some polymer pairs we have found that it was not practically possible to take cloud point measurements, without thermal degradation and/or cross-linking reactions, using PS/PI or PS/PB pairs that have molecular weights comparable to the molecular weights of the SI or SB diblock copolymers reported in the literature.[8−11] In this regard, the predicted T_{ODT}'s of SI or SB diblock copolymers and their saturated counterparts, which will be presented later in this paper, must be regarded as being only a useful guideline, showing a general trend (i.e., increasing or decreasing trend) when the expressions for the segment−segment interaction parameter were obtained from lower molecular weights of PS/PI, PVCH/PEP, PS/PB, or PVCH/PEB pairs. Later in this paper we will elaborate on this further.

Figure 2 gives phase diagrams of (PS-6)/(PI^{1,4}-5), (PVCH-6)/(PI^{1,4}-5), (PS-6)/(PEP^{1,4}-5), and (PVCH-6)/(PEP^{1,4}-5) blends, all showing upper critical solution temperature (UCST). The molecular weights of the constituent components in all four polymer pairs are kept nearly constant.

It is seen from Figure 2 that the T_c of the (PVCH-6)/(PI^{1,4}-5) blends is slightly lower than that of the (PS-6)/(PI^{1,4}-5) blends, indicating that the segment−segment interaction between PVCH-6 and PI^{1,4}-5 is *less* repulsive than that between PS-6 and PI^{1,4}-5; the saturation of PS to PVCH has *increased* the miscibility of the (PS-6)/(PI^{1,4}-5) blends. On the other hand, in Figure 2 we observe that the T_c of the (PS-6)/(PEP^{1,4}-5) blends is much higher than that of the (PS-6)/(PI^{1,4}-5) blends, indicating that the segment−segment interaction between PS-6 and PEP^{1,4}-5 has become much more repulsive after the saturation of PI^{1,4}-5; the saturation of PI^{1,4} to PEP^{1,4} has *decreased* the miscibility of the (PS-6)/(PI^{1,4}-5) blends. It is interesting to observe in Figure 2 that the binodal curve of the (PVCH-6)/(PEP^{1,4}-5) blends lies slightly above that of the (PS-6)/(PI^{1,4}-5) blends, suggesting that the T_{ODT} of the PVCH-*block*-PEP copolymer will be higher than that of the unsaturated precursor. Further, Figure 2 indicates that the net effect of saturation of both PS and PI on the miscibility of PVCH/PEP pair is determined more by the saturation of PI than the saturation of PS. The above observations now explain qualitatively why the T_{ODT}'s of PVCH-*block*-PEP^{1,4} copolymers reported in the literature[8−11] are increased over those of the unsaturated precursors having a PI block with predominantly 1,4-addition. Below we will estimate, via mean-field theory,[5] the T_{ODT}'s of the PVCH-*block*-PEP^{1,4} copolymers reported in the literature.[8−11] The phase diagrams presented above lead us to conclude that the miscibility of the PS/PI pair having a PI with predominantly 1,4-addition or its saturated counterpart increases in the order PS/PEP^{1,4} < PVCH/PEP^{1,4} < PS/PI^{1,4} < PVCH/PI.^{1,4}

Figure 3 describes the effect of molecular weight on the binodal curves of PS/PI^{1,4} and PVCH/PEP^{1,4} blends, showing that the binodal curves of both PS/PI^{1,4} and PVCH/PEP^{1,4} blends move upward as the molecular weights of the constituent components are increased, indicating that the segment−segment interactions between PS and PI and between PVCH and PEP become more repulsive as the molecular weight is increased. The above observation suggests, once again, that it is very important to have the same or approximately the same polymerization index to compare the segment−segment interaction parameter (or miscibility) of one polymer pair with another pair.

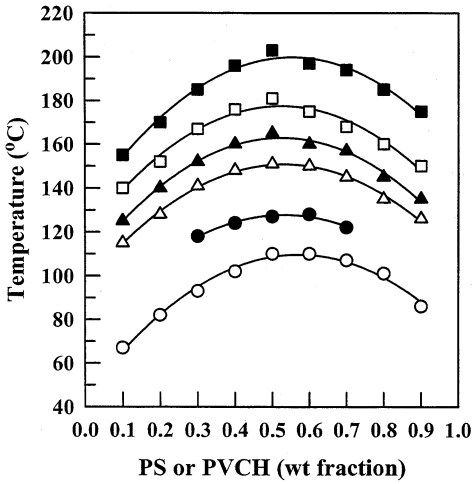

Figure 3. Phase diagrams for (○) (PS-2)/(PI^{1,4}-5) blends with T_c = 110 °C, (●) (PVCH-2)/(PEP^{1,4}-5) blends with T_c = 127 °C, (△) (PS-6)/(PI^{1,4}-5) blends with T_c = 151 °C, (▲) (PVCH-6)/(PEP^{1,4}-5) blends with T_c = 165 °C, (□) (PS-6)/(PI^{1,4}-10) blends with T_c = 181 °C, and (■) (PVCH-6)/(PEP^{1,4}-10) blends with T_c = 203 °C.

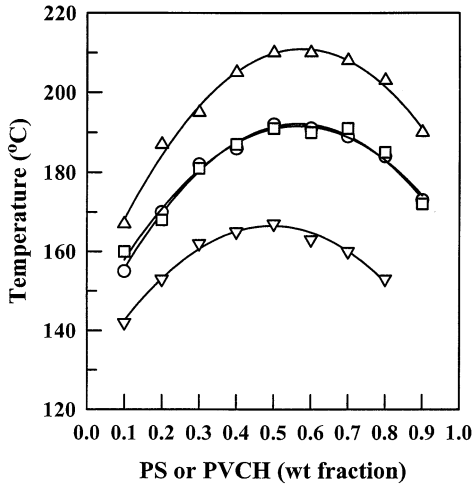

Figure 4. Phase diagrams for (○) (PS-2)/(PI^{3,4}-6) blends with T_c = 192 °C, (△) (PS-2)/(PEP^{3,4}-6) blends with T_c = 210 °C, (□) (PVCH-10)/(PI^{3,4}-6) blends with T_c = 191 °C, and (▽) (PVCH-10)/(PEP^{3,4}-6) blends with T_c = 167 °C.

Phase Diagrams of PS/PI^{3,4} and PVCH/PEP^{3,4} Blends. Figure 4 gives phase diagrams of (PS-2)/(PI^{3,4}-6), (PS-2)/(PEP^{3,4}-6), (PVCH-10)/(PI^{3,4}-6), and (PVCH-10)/(PEP^{3,4}-6) blends, where PI^{3,4}-6 has high vinyl content, 59% 3,4-addition and 34% 1,2-addition (see Table 1). The T_c of the (PS-2)/(PI^{3,4}-6) blends is 192 °C (Figure 4) while the T_c of the (PS-2)/(PI^{1,4}-5) blends is only 110 °C (Figure 1), indicating that the (PS-2)/(PI^{3,4}-6) blends are far less miscible than the (PS-2)/(PI^{1,4}-5) blends, even though the molecular weight of PI^{3,4}-6 is only slightly higher than that of PI^{1,4}-5. That is, the microstructure of PI has a profound influence on its miscibility with PS. In Figure 4 we observe that the T_c of the (PS-2)/(PEP^{3,4}-6) blends is increased to 210 °C when PI^{3,4}-6 is saturated, yielding PEP^{3,4}-6.

However, when PS-2 was saturated and mixed with PI^{3,4}-6, the miscibility of the (PVCH-2)/ (PI^{3,4}-6) blends was so good that the blends were clear even at room temperature over the entire range of blend compositions. PVCH-2 has a T_g of 63 °C, and thus we can state that the T_c of the (PVCH-2)/(PI^{3,4}-6) blends lies below 63 °C. We made the same observations with the (PVCH-3)/(PI^{3,4}-6) and (PVCH-6)/(PI^{3,4}-6) blends, and finally we were able to observe cloud points when the molecular weight of PVCH was increased to ca. 10^4 g/mol, yielding (PVCH-10)/(PI^{3,4}-6) blends. In Figure 4 we observe that the phase diagram of (PVCH-10)/(PI^{3,4}-6) blends (the symbol □) almost overlaps the phase diagram of the (PS-2)/(PI^{3,4}-6) blends (the symbol ○), and the miscibility of the (PVCH-10)/(PEP^{3,4}-6) blends (the symbol ▽) becomes even greater than that of the (PVCH-10)/ (PI^{3,4}-6) blends (Figure 4), while the T_c of the (PVCH-10)/(PEP^{3,4}-6) blends is 167 °C, 25 °C lower than the T_c of the (PS-2)/(PI^{3,4}-6) blends (the symbol ○). The observation made in Figure 4 for the PVCH/PEP^{3,4} blends is opposite to that made in Figure 2 for the PVCH/PEP^{1,4} blends, suggesting that the T_{ODT} of PVCH-*block*-PEP^{3,4} copolymer will be lower than that of the unsaturated precursor, SI^{3,4} diblock copolymer. To date, no experimental study has been reported on the T_{ODT} of PVCH-*block*-PEP^{3,4} copolymer. The phase diagrams presented in Figure 4 lead us to conclude that the miscibility of the PS/PI pair having a PI with high vinyl content or its saturated counterpart increases in the order PS/PEP^{3,4} < PS/PI^{3,4} < PVCH/PI^{3,4} < PVCH/PEP.^{3,4}

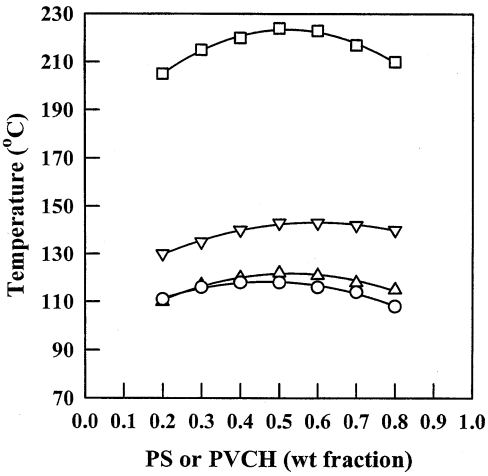

Figure 5. Phase diagrams for (○) (PS-2)/(PB^{1,4}-26H) blends with T_c = 118 °C, (△) (PVCH-2)/(PB^{1,4}-26H) blends with T_c = 122 °C, (□) (PS-2)/(PEB^{1,4}-26H) blends with T_c = 224 °C, and (▽) (PVCH-2)/(PEB^{1,4}-26H) blends with T_c = 143 °C.

Phase Diagrams of PS/PB^{1,4} and PVCH/PEB^{1,4} Blends. Figure 5 gives phase diagrams of (PS-2)/(PB^{1,4}-26H), (PVCH-2)/(PB^{1,4}-26H), (PVCH-2)/(PEB^{1,4}-26H), and (PS-2)/(PEB^{1,4}-26H) blends, in which PB^{1,4}-26H has predominantly (74%) 1,4-addition (see Table 1) and PEB^{1,4}-26H is the saturated counterpart of PB^{1,4}-26H. Notice that the molecular weights of the components in the above blends are kept almost the same. We used PB^{1,4}-26H instead of PB^{1,4}-7H (having 93% 1,4-addition) because PEB^{1,4}-7H (obtained by the saturation of PB^{1,4}-7H) became highly crystalline (almost like a polyethylene) upon hydrogenation. For this reason, it did not dissolve in a common solvent (toluene) for preparation of binary blends with PVCH by solvent casting. On the other hand, PEB-26H, after the saturation of PB-26H, was found to dissolve in toluene, enabling us to prepare binary blends with PVCH by solvent casting.

The following observations are worth noting in Figure 5. The T_c of (PVCH-2)/(PB^{1,4}-26H) blends is slightly higher than that of the (PS-2)/(PB^{1,4}-26H) blends, indicating that the segment−segment interaction between PVCH-2 and PB^{1,4}-26H is *more or less* the same as that between PS-2 and PB^{1,4}-26H; the saturation of

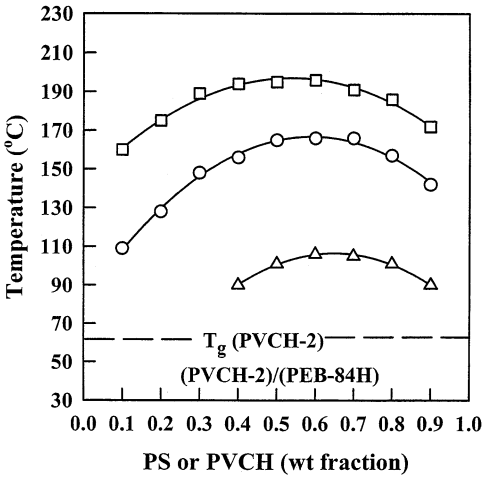

Figure 6. Phase diagrams for (○) (PS-2)/(PB^{1,2}-84H) blends with T_c = 165 °C, (△) (PVCH-2)/(PB^{1,2}-84H) blends with T_c = 106 °C, (□) (PS-2)/(PEB^{1,2}-84H) blends with T_c = 195 °C, and (PVCH-2)/(PEB^{1,2}-84H) blends have T_c < 63 °C.

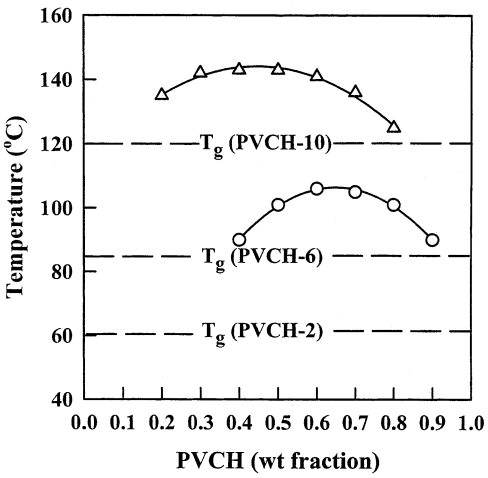

Figure 7. Phase diagrams for (○) (PVCH-2)/(PB^{1,2}-84H) blends with T_c = 106 °C and (△) (PVCH-10)/(PEB^{1,2}-84H) blends with T_c = 143 °C. The (PVCH-2)/(PEB^{1,2}-84H) and (PVCH-6)/(PEB^{1,2}-84H) blends did not show turbidity at room temperature, indicating that the critical temperature (T_c) of the (PVCH-2)/(PEB^{1,2}-84H) blends was below the glass transition temperature (T_g = 63 °C) of PVCH-2 and the T_c of the (PVCH-6)/(PEB^{1,2}-84H) blends was below the T_g (83 °C) of PVCH-6.

PS has changed very *little* the miscibility of the (PVCH-2)/(PB^{1,4}-26H) blends. On the other hand, in Figure 5 we observe that the T_c of the (PS-2)/(PEB^{1,4}-26H) blends has increased more than 100 °C over that of (PS-2)/(PB^{1,4}-26H) blends, indicating that the segment−segment interaction between PS-2 and PEB^{1,4}-26H has become strongly repulsive compared to that between PS-2 and PB^{1,4}-26H; the saturation of PB^{1,4}-26H has decreased dramatically the miscibility of the (PS-2)/(PEB^{1,4}-26H) blends. Such a dramatic decrease in miscibility of the (PS-2)/(PEB^{1,4}-26H) pair is attributable to the formation of polyethylene (PE) from the saturation of the 1,4-addition in PB^{1,4}-26H. In Figure 5, we observe that after the saturation of both PS-2 and PB^{1,4}-26H the T_c of the (PVCH-2)/(PEB^{1,4}-26H) blends has increased by 25 °C over that of the unsaturated precursor, but the increase is not as large at that observed in the (PS-2)/(PEB^{1,4}-26H) blends. The phase diagrams given in Figure 5 lead us to conclude that the miscibility of the PS/PB pair having a PB with predominantly 1,4-addition or its saturated counterpart increases in the order PS/PEB^{1,4} ≪ PVCH/PEB^{1,4} < PVCH/PB^{1,4} ≈ PS/PB.[1,4] The above observations now explain qualitatively why the T_{ODT} of PE-PVCHd-1 reported by Gehlsen and Bates[9] and the T_{ODT} of VCH/E−62 reported by Adams et al.,[10] both PE-PVCHd-1 and VCH/E−62 being PVCH-*block*-PEB^{1,4} copolymer, increased dramatically (124−140 °C) over that of the unsaturated precursors.

Phase Diagrams of PS/PB^{1,2} and PVCH/PEB^{1,2} Blends. Figure 6 gives phase diagrams of (PS-2)/(PB^{1,2}-84H), (PVCH-2)/(PB^{1,2}-84H), and (PS-2)/(PEB^{1,2}-84H) blends. Note that PB-84H has predominantly (84%) 1,2-addition (see Table 1), and PEB^{1,2}-84H is the saturated counterpart of PB^{1,2}-84H. It should be mentioned that (PVCH-2)/(PEB^{1,2}-84H) blends were clear at room temperature over the entire range of blend compositions tested, and PVCH-2 has a T_g of 63 °C. Thus, we can state that the T_c of the (PVCH-2)/(PEB^{1,2}-84H) blends lies below 63 °C, as indicated in Figure 6.

The following observations are worth noting in Figure 6. The T_c of the (PVCH-2)/(PB^{1,2}-84H) blends is below 106 °C, indicating that the segment−segment interaction between PVCH-2 and PB^{1,2}-84H is *less* repulsive than that between PS-2 and PB^{1,2}-84H; the saturation of PS has led to a pronounced *increase* in the miscibility of PVCH/PB^{1,2} blends over that of PS/PB^{1,2} blends. On the other hand, in Figure 6 we observe that the T_c of (PS-2)/(PEB^{1,2}-84H) blends has increased by 30 °C over that of the (PS-2)/(PB^{1,2}-84H) blends. This increase in T_c for the (PS-2)/(PEB^{1,2}-84H) blends is much smaller than that observed for the (PS-2)/(PB^{1,4}-26H) blends (see Figure 5), indicating that the segment−segment interaction between PS-2 and PEB^{1,2}-84H is much *less* repulsive than that between PS-2 and PEB^{1,2}-26H (compare Figure 6 with Figure 5). What is of great interest in Figure 6 is that the saturation of both PS-2 and PB^{1,2}-84H has *increased* dramatically the miscibility of the unsaturated precursor. Figure 7 describes the effect of the molecular weight of PVCH on the phase behavior (i.e., miscibility) of PVCH/(PEB^{1,2}-84H) blends, showing that T_c increases as the molecular weight of PVCH is increased.

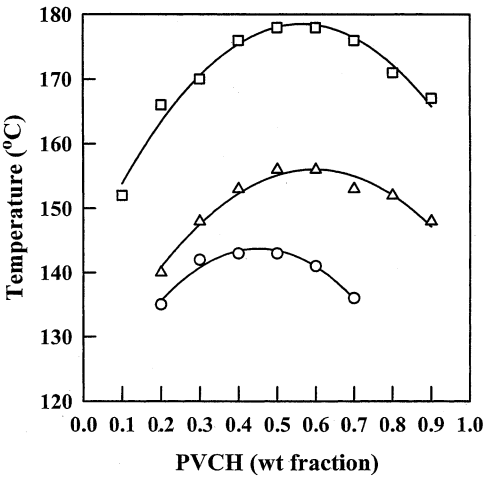

Figure 8. Phase diagrams for (○) (PVCH-10)/(PEB^{1,2}-84H) blends with T_c = 143 °C, (△) (PVCH-10)/(PEB^{1,2}-50H) blends with T_c = 156 °C, and (□) (PVCH-10)/(PEB^{1,2}-26H) blends with T_c = 178 °C.

Figure 8 describes the effect of the microstructure of PEB on the miscibility of PVCH/PEB blends, in which PEB^{1,2}-50H has 50% 1-butene content. It is clearly seen in Figure 8 that the miscibility between PVCH and

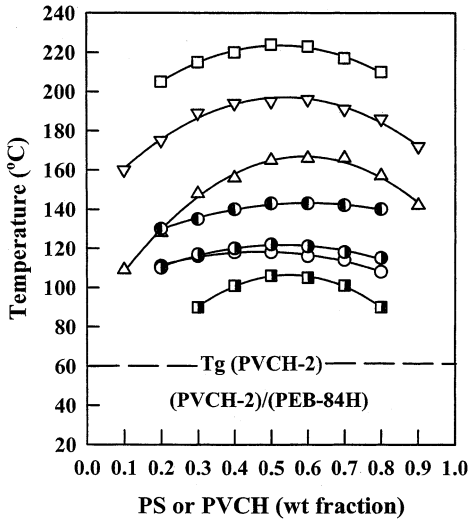

Figure 9. Phase diagrams for (○) (PS-2)/($PB^{1,2}$-26H) blends with T_c = 118 °C, (△) (PS-2)/($PB^{1,2}$-84H) blends with T_c = 165 °C, (□) (PS-2)/($PEB^{1,2}$-26H) blends with T_c = 224 °C, (▽) (PS-2)/($PEB^{1,2}$-84H) blends with T_c = 195 °C, (◑) (PVCH-2)/($PB^{1,2}$-26H) blends with T_c = 122 °C, (◨) (PVCH-2)/($PB^{1,2}$-84H) blends with T_c = 106 °C, and (◐) (PVCH-2)/($PEB^{1,2}$-26H) blends with T_c = 143 °C. The (PVCH-2)/($PEB^{1,2}$-84H) blends did not show turbidity at room temperature, indicating that the T_c of the blends was below the T_g (63 °C) of PVCH-2.

$PEB^{1,2}$ increases as the 1-butene content in PEB increases. The above observations suggest that the T_{ODT} of PVCH-*block*-$PEB^{1,2}$ copolymer will decrease as the 1-butene content in the PEB block is increased, meaning that the T_{ODT} of PVCH-*block*-$PEB^{1,2}$ copolymer will be *lower* than that of the unsaturated precursor having a PB block with predominantly 1,2-addition. Gehlsen and Bates[9] indeed reported that the T_{ODT} of a PVCH-*block*-$PEB^{1,2}$ copolymer was *lower* than that of the unsaturated precursor having a PB block with predominantly 1,2-addition. Thus, we can conclude that the experimentally observed dramatic increase (124−140 °C) in T_{ODT} of PEPVCHd-1[9] and VCH/E−62,[10] which are PVCH-*block*- $PEB^{1,4}$ copolymer, should not be regarded as being a general physical phenomenon for all block copolymers obtained from the saturation of SB diblock copolymer. In other words, the T_{ODT} of PVCH-*block*-PEB copolymer can be higher or lower than that of the unsaturated precursor, depending upon the microstructures of the PB block in an SB diblock copolymer. The phase diagrams given in Figures 6 and 8 lead us to conclude that the miscibility of the PS/PB pair having a PB with predominantly 1,2-addition or its saturated counterpart increases in the order PS/$PEB^{1,2}$ < PS/$PB^{1,2}$ < PVCH/$PB^{1,2}$ ≪ PVCH/ $PEB.^{1,2}$ The above inequalities for the PVCH/$PEB^{1,2}$ blends are quite different from those for the PVCH/$PEB^{1,4}$ blends.

Figure 9 gives composite phase diagrams describing the effect of microstructures of PB on the miscibility of PS/$PB^{1,2}$ and PS/$PB^{1,4}$ blends and also on the miscibility of saturated counterparts, PVCH/$PEB^{1,2}$ and PVCH/ $PEB^{1,4}$ blends. From Figure 9 we conclude that the miscibility of PS/PB pairs having a PB with predominantly 1,2- or 1,4-addition, and their saturated counterparts increases in the order PS/$PEB^{1,4}$ < PS/$PEB^{1,2}$ < PS/$PB^{1,2}$ < PVCH/$PEB^{1,4}$ < PVCH/$PB^{1,4}$ ≈ PS/$PB^{1,4}$ < PVCH/$PB^{1,2}$ ≪ PVCH/$PEB.^{1,2}$

Determination of the Interaction Parameters for the Polymer Pairs Investigated in This Study. In many studies the following form of a simple expression for the interaction parameter χ

$$\chi = a + b/T \tag{1}$$

where a and b are constants, has been obtained by curve fitting the experimental data from cloud point measurements of binary blends to the Flory−Huggins theory or the experimental data from small-angle X-ray scattering (SAXS) or small-angle neutron scattering (SANS) of diblock copolymers to the random phase approximation theory of Leibler.[5]

We are well aware of the fact that the miscibility (i.e., χ) of a polymer pair very much depends on the molecular weights of the constituent components. Therefore, it would have been ideal if we could take cloud point measurements for PS/PI, PVCH/PEP, PS/PB, and PVCH/PEB pairs by varying the molecular weight of the various homopolymers or choosing the molecular weights of various hompolymers that are very close to the molecular weights of the constituent components of the SI diblock copolymers, PVCH-*block*-PEP copolymers, SB diblock copolymer, and PVCH-*block*-PEB copolymer reported in the literature.[8−11] As mentioned above, however, in carrying out cloud point measurements, we had very limited choices for varying the molecular weights of the constituent components for PS/PI, PS/PB, PVCH/PEP, and PVCH/PEB pairs for the following practical reasons. To have the same or approximately the same molecular weight for PS/PI and PVCH/PEP blends and for PS/PB and PVCH/PEB blends, we had to choose relatively low molecular weights of the homopolymers. In some polymer pairs, even this was not possible. For instance, the T_c of the (PS-2)/($PB^{1,2}$-84H) blends was 186 °C, which is very close to the thermal degradation/cross-linking temperature of $PB^{1,2}$-84H, while the miscibility of the saturated counterpart, (PVCH-2)/($PEB^{1,2}$-84H) blends, was so good that we could not determine cloud points for the polymer pair. Thus, we had to increase the molecular weight of PVCH until we could measure the T_c of the binary blends. It turned out that, by increasing the molecular weight of PVCH to ca. 10^4 g/mol, we were able to measure the T_c of the (PVCH-10)/($PEB^{1,2}$-84H) blends. On the other hand, the T_c of the unsaturated counterpart, (PS-10)/ ($PB^{1,2}$-84H) blends, exceeded 220 °C, which is far above the thermal degradation/cross-linking temperature of $PB^{1,2}$-84H. Thus, we could not measure the cloud points of PS/$PB^{1,2}$ and PVCH/$PEB^{1,2}$ blends having identical molecular weights. The same situation arose for other polymer pairs employed in this study.

In the present study we obtained expressions for the interaction parameter α (having the units of mol/cm^3) in the following form

$$\alpha = a + b/T + c\phi_1/T \tag{2}$$

where a, b, and c are constants, ϕ_1 is the volume fraction of component 1, and T is the absolute temperature, by curve-fitting the experimental phase diagrams to theoretical phase diagrams predicted from the Flory−Huggins theory. The readers are referred to the literature[14,17] that describes the rationale behind the choice of the form given by eq 2. The Flory−Huggins interaction parameter χ can be determined from the relationship $\chi = \alpha V_r$ with V_r being the molar volume of a

Table 3. Interaction Parameters for PS/PI, PS/PB, PVCH/PEP, and PVCH/PEB Pairs Determined by Cloud Point Measurement

sample code	interaction parameter α (mol/cm^3)[a]	eq no.
	(a) PS/PI^{1,4} and PVCH/PEP^{1,4} Blends	
(PS-6)/(PI^{1,4}-5)	$\alpha = -0.1261 \times 10^{-2} + 0.6497/T + 0.0168\phi_{PS}/T$	5
(PVCH-6)/(PEP^{1,4}-5)	$\alpha = -0.9884 \times 10^{-3} + 0.5587/T - 0.0333\phi_{PVCH}/T$	6
	(b) PS/PI^{3,4} and PVCH/PEP^{3,4} Blends	
(PS-2)/(PI^{3,4}-6)	$\alpha = -0.2904 \times 10^{-2} + 1.6081/T - 0.0576\phi_{PS}/T$	7
(PVCH-10)/(PEP^{3,4}-6)	$\alpha = -0.1085 \times 10^{-2} + 0.5660/T - 0.0057\phi_{PVCH}/T$	8
	(c) PS/PB^{1,4} and PVCH/PEB^{1,4} Blends	
(PS-2)/(PB^{1,4}-26H)	$\alpha = -0.5345 \times 10^{-2} + 2.4001/T - 0.1306\phi_{PS}/T$	9
(PVCH-10)/(PEB^{1,4}-26H)	$\alpha = -0.2419 \times 10^{-2} + 1.1734/T + 0.0887\phi_{PVCH}/T$	10
	(d) PS/PB^{1,2} and PVCH/PEB^{1,2} Blends	
(PS-2)/(PB^{1,2}-84H)	$\alpha = -0.2076 \times 10^{-2} + 1.1182/T - 0.0051\phi_{PS}/T$	11
(PVCH-10)/(PEB^{1,2}-84H)	$\alpha = -0.1028 \times 10^{-2} + 0.5097/T + 0.0069\phi_{PVCH}/T$	12

[a] The Flory−Huggins interaction parameter χ is related to α by $\chi = \alpha V_r$ with V_r being the molar volume of reference component.

Table 4. Expressions for the Specific Volumes of PS, PI, PB, PEB, PEP, and PVCH Employed for the Calculation of Reference Volume *V*

material	specific volume (cm^3/g)	ref
PS	$v_{PS} = 0.9217 + 5.412 \times 10^{-4}(T - 273) + 1.687 \times 10^{-7}(T - 273)^2$	18
PI	$v_{PI} = 1.0771 + 7.22 \times 10^{-4}(T - 273) + 2.46 \times 10^{-7}(T - 273)^2$	14
PB	$v_{PB} = 1.1072 + 8.19 \times 10^{-4}(T - 273)$	14
PEB	$v_{PEB} = 1.134 + 7.003 \times 10^{-4}(T - 273)$	14
PEP	$v_{PEP} = 1.2061 + 9.69 \times 10^{-4}(T - 406)$	this study
PVCH	$v_{PVCH} = 1.0084 + 6.541 \times 10^{-4}(T - 273)$	this study[a]

[a] The details of the experimental procedures employed to obtain the specific volume for PVCH are described in ref 19.

reference component. It should be mentioned that there are different ways of defining V_r, for instance,

$$V_r = [M]_1 v_1 \tag{3}$$

or

$$V_r = [([M]_1 v_1)([M]_2 v_2)]^{1/2} \tag{4}$$

where $[M]_1$ and $[M]_2$ are the monomeric molecular weights of components 1 and 2, respectively, and v_1 and v_2 are the specific volumes of components 1 and 2, respectively. Table 3 gives a summary of the expressions of α for PS/PI^{1,4}, PVCH/PEP^{1,4}, PS/PI^{3,4}, PVCH/PEP^{3,4}, PS/PB^{1,4}, PVCH/PEB^{1,4}, PS/PB^{1,2}, and PVCH/PEB^{1,2} pairs thus determined.

Prediction of the T_{ODT}'s of PVCH-*block*-PEP and PVCH-*block*-PEB Copolymers and Their Unsaturated Precursors. Using the Leibler theory,[5] together with the expressions for α given in Table 3, we predicted the T_{ODT}'s of the PVCH-*block*-PEP and PVCH-*block*-PEB copolymers and their unsaturated precursors having PI or PB blocks with predominantly 1,4-addition reported by various research groups in the literature[8,10,11] and then compared them with experimental results. In so doing, we used eq 4 to calculate V_r and then χ from $\chi = \alpha V_r$, for which the expressions for the temperature-dependent specific volumes given in Table 4 for PS, PI, PB, PEB, PEP, and PVCH were used. We wish to point out that the predicted T_{ODT} of a block copolymer is very sensitive to the choice of the expressions for χ (or α); different values of T_{ODT} may be predicted when using different expressions for the interaction parameter. It is appropriate to mention at this juncture that while the expressions for α summarized in Table 3 were obtained using binary blends, extending the lattice cluster theory,[20,21] Freed and co-workers[22,23] have shown that the χ for a block copolymer would not be the same as that for the corresponding binary blends, because end effects associated with junction point in diblock copolymer chains might play an important role in the determination of the segment−segment interaction parameter for diblock copolymers. According to Freed and co-workers,[22,23] the differences in χ's between the blend and diblock copolymer are manifested by the opposite temperature dependence when polymerization index N is included in obtaining the following form of expression

$$\chi = (a + b/N) + (c + d/N)/T \tag{13}$$

where a, b, c, and d are constants and T is the absolute temperature; i.e., they emphasized the importance of including molecular weight in the expression for χ. Notice that eq 13 reduces to eq 1 for very large values of N. The readers are reminded that above we already have mentioned the practical difficulty with measuring cloud points for PS/PI pairs, for example (see Figure 1), having very high molecular weights, enabling us to determine values of a, b, c, and d appearing in eq 13. Therefore, the discussion below should be regarded as being qualitative, and our purpose here is to focus on the general trend.

Table 5 gives a summary of the predicted T_{ODT}'s and experimental results for five PVCH-*block*-PEP copolymers[8,10,11] and one PVCH-*block*-PEB copolymer.[10] It can be seen in Table 5 that the predicted values of T_{ODT} for the PVCH-*block*-PEP and PVCH-*block*-PEB copolymers are higher than those of the unsaturated precursors having PI or PB blocks with predominantly 1,4-addition, confirming the experimental results. Interestingly, the predicted difference in T_{ODT}, ΔT_{ODT}, before and after the complete saturation of an SI diblock copolymer (PVCH−PEP-2 and VCH/EP series) is reasonably close to that reported experimentally, while the predicted values of T_{ODT} are much lower than the experimentally measured ones. On the other hand, the predicted ΔT_{ODT} between PVCH-*block*-PEB copolymer (VCH/E-62) and the unsaturated precursor (S/B-62) is considerably less than that reported experimentally.

Table 5. Summary of the Measured and Predicted T_{ODT}'s for the SI, SB, PVCH-*block*-PEP, and PVCH-*block*-PEB Copolymers in the Literature

sample code	$M_w \times 10^{-3}$ (g/mol)	wt fract of PS or PVCH	measd T_{ODT} (°C)	ref	predicted T_{ODT} (°C)
		(a) SI Diblock and PVCH-*blolck*-PEP Copolymers			
PS−PI-2[a]	18.0	0.500	124 ± 2	8	66
PVCH−PEP-2	18.6	0.502	140 ± 2	8	92
S/I-90[b]	90.6	0.131	202 ± 2	10	78
VCH/EP-90	93.6	0.134	234 ± 3	10	104
S/I 10/15[c]	24.4	0.393	149 ± 1	11	99
VCH/EP 10/15	25.3	0.398	164 ± 2	11	120
S/I 10/16[c]	25.6	0.378	171 ± 1	11	101
VCH/EP 10/16	26.6	0.385	178 ± 2	11	122
S/I 8/17[c]	25.2	0.335	158 ± 1	11	80
VCH/EP 8/17	26.2	0.341	170 ± 2	11	106
		(b) SB Diblock and PVCH-*block*-PEB Copolymer			
S/B-62[b]	62.0	0.124	107 ± 3	10	108
VCH/E-62	64.5	0.126	231 ± 3	10	129

[a] 95% 1,4-addition in PI. [b] High 1,4-diene addition but the amount of 1,4-addition was not specified. [c] 6.5−7.2% 3,4-addition in PI.

In Table 5 we have not included the experimental results of Balsara et al.,[12] because their results are complicated by the close proximity of T_g and T_{ODT} for the PVCH-*block*-PEP copolymer they studied. The SI diblock copolymer they characterized underwent a glass transition beginning at 61 °C and ending at 71 °C, and the T_{ODT} as determined by small-angle neutron scattering (SANS) was 77 °C. The reported value of T_{ODT} is very close to the T_g of the block copolymer, which complicates accurate measurement of the T_{ODT}. Balsara et al. also reported that the T_{ODT} as determined by SANS and also by birefringence of the saturated counterpart (HSHI) of their SI diblock copolymer was 70 °C, 7 °C below the T_{ODT} of the unsaturated precursor. Because the T_{ODT} of HSHI lies inside the glass transition region which, according to Balsara et al., begins at 68 °C and ends at 90 °C. The T_{ODT} of this block copolymer cannot be measured accurately in this temperature range. In view of the fact that the microstructures of PI block in their SI diblock had predominantly (93%) 1,4-addition, it would not be possible to have the T_{ODT} of a PVCH-*block*-PEP copolymer lower than that of the unsaturated precursor (see the phase diagrams given in Figure 2). Using the Leibler theory and the expressions for α given by eqs 5 and 6 in Table 3, we estimate the T_{ODT} of their SI diblock copolymer to be 64 °C and the T_{ODT} of the saturated counterpart (HSHI) to be 68 °C. Consistent with the predictions made for the five PVCH-*block*-PEP copolymers given in Table 5, mean-field theory at least predicts an increasing trend of T_{ODT} after saturation of the SI diblock copolymer of Balsara et al.[12] Nevertheless, the predicted values of T_{ODT} are of no physical significance when they lie in the vicinity of or far below the T_g of the block copolymer. It should be pointed out that mean-field theory does not take into account the T_g effect.

In the present study we measured the T_g of PVCHs having different molecular weights, the results of which are given in Figure 10. Using the midpoint of glass transition given in Figure 10, we have prepared Figure 11, describing the effect of molecular weight of PVCH on T_g. In Figure 11 we observe that the T_g of PVCH increases linearly with molecular weight until reaching approximately 13 kg/mol and then levels off. Our result summarized in Figure 11 is in good agreement with the previous study of Hahn and co-workers.[13] As already mentioned with reference to Figure 7, we could not determine cloud points of PVCH/PEB[1,2] blends until the molecular weight of PVCH was increased to 10 kg/mol at a fixed molecular weight of ca. 3.8 kg/mol for PEB.[1,2]

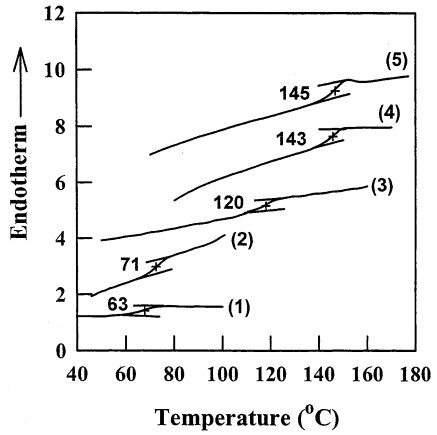

Figure 10. DSC traces for PVCH with varying molecular weights: (1) M_n = 2000 g/mol, (2) M_n = 3000 g/mol, (3) M_n = 10 000 g/mol, (4) M_n = 13 000 g/mol, and (5) M_n = 18 000 g/mol.

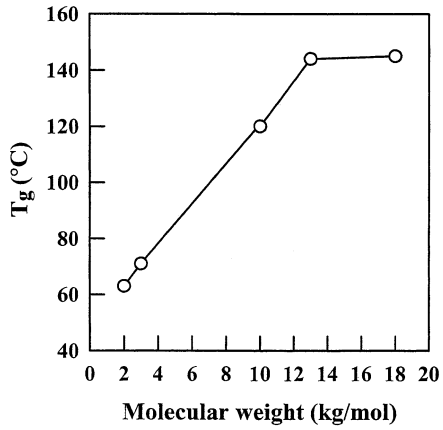

Figure 11. Plot of T_g vs molecular weight of PVCH.

This is because the miscibility between PVCH and PEB[1,2] is so good that the cloud points lie *below* the T_g of PVCH until its molecular weigh reaches 10 kg/mol (see Figure 7). On the other hand, as given in Figure 12, we were able to construct phase diagrams of the PVCH/PEP[1,4] blends for the molecular weight of PVCH as low as 2 kg/mol at a fixed molecular weight of ca. 5 kg/mol for PEP,[1,4] because the cloud points of each blend lie *above* the T_g of PVCH in the respective blend. We therefore conclude that the experimental determination of T_{ODT} of PVCH-*block*-PEP or PVCH-*block*-PEB copolymers would be possible only when T_{ODT} lies well above the T_g of PVCH block in the respective block copolymer.

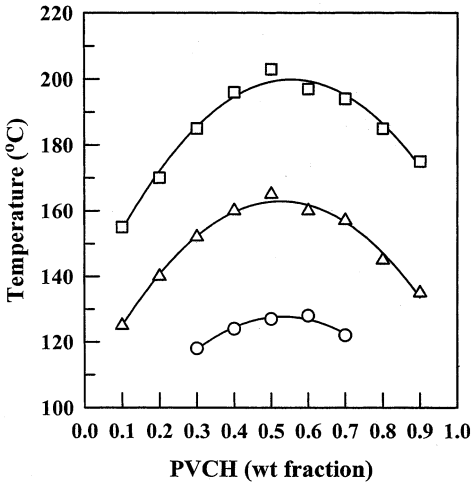

Figure 12. Phase diagrams for (○) (PVCH-2)/(PEP^{1,4}-5) blends with T_c = 127 °C, (△) (PVCH-6)/(PEP^{1,4}-5) blends with T_c = 165 °C, and (□) (PVCH-6)/(PEP^{1,4}-10) blends with T_c = 203 °C.

4. Concluding Remarks

In this study we have found that the saturation of PI,^{1,4} yielding PEP,^{1,4} increases repulsive segment−segment interaction between PS and PEP,^{1,4} while the saturation of PS decreases repulsive segment−segment interaction between PVCH and PI,^{1,4} as compared to the segment−segment interaction between PS and PI.^{1,4} We have found a similar trend when a PB^{1,4} was saturated to obtain PEB^{1,4} and then investigated segment−segment interaction between PS and PEB^{1,4} and between PVCH and PB^{1,4} blends. Our experimental results show that the extent of an increase in repulsive segment−segment interactions after the saturation of PI^{1,4} (or PB^{1,4}) is *not* the same as the extent of a decrease in repulsive segment−segment interactions after the saturation of PS. Therefore, the segment−segment interaction between PVCH and PEP^{1,4} relative to that between PS and PI^{1,4} and the segment−segment interaction between PVCH and PEB^{1,4} relative to that between PS and PB^{1,4} would depend on the effectiveness of the saturation of PS vs the effectiveness of the saturation of PI^{1,4} (or PB^{1,4}). The above observations can be extended to SI or SB diblock copolymers before and after the saturation, yielding PVCH-*block*-PEP or PVCH-*block*-PEB copolymers. Using the results of cloud point measurements, we have constructed phase diagrams and then determined the segment−segment interaction parameter for several polymer pairs associated with SI, SB, PVCH-*block*-PEP, and PVCH-*block*-PEB copolymers. We successfully explained the origin of an increase in T_{ODT} of the PVCH-*block*-PEP or PVCH-*block*-PEB copolymers over the T_{ODT} of the unsaturated precursors having PI or PB blocks with predominantly 1,4-addition.

In the present study we have investigated the phase behavior of PS/PI and PS/PB blends with varying microstructures (i.e., low or high vinyl contents) of PI or PB and found that the microstructures of polydiene play a significant role in determining the segment−segment interaction parameter (i.e., miscibility) of PS/PI and PS/PB blends. Specifically, our study indicates (see Figure 9) that the critical temperature in the binodal curve of PS/PB blend increases (thus the miscibility decreases) as the amount of 1,2-addition in PB increases (i.e., the PB having high 1,2-addition is less miscible with PS than the PB having high 1,4-addition), while the critical temperature of the binodal curve for PVCH/PEB blend decreases (thus the miscibility increases) as the amount of 1-butene in PEB increases, and the critical temperature of the PVCH/PEB^{1,2} blend is even lower than that of the unsaturated precursor, PS/PB^{1,2} blends. Using mean-field theory and the expression for the segment−segment interaction parameter given Table 3, we estimated the T_{ODT} of PVCH-*block*-PEB copolymers with very high or low 1-butene contents in the PEB block. We found that the predicted T_{ODT} of PVCH-*block*-PEB copolymer with high 1-butene content in the PEB block is lower than that of the unsaturated precursor. This prediction is consistent with the experimental findings of Gehlsen and Bates.[9] The predicted T_{ODT} of PVCH-*block*-PEP copolymer with high vinyl content in the PEP block has shown a similar trend. However, at present there are *no* experimental data reported in the literature on the T_{ODT} of PVCH-*block*-PEP copolymer with high vinyl content in the PEP block. We conclude that the T_{ODT} of PVCH-*block*-PEP and PVCH-*block*-PEB copolymers can be higher or lower than that of the unsaturated precursors, depending upon the microstructures of the polydiene block in the SI or SB diblock copolymers.

One of the most interesting observations made in this study is that the repulsive segment−segment interactions between PVCH and PEP^{3,4} having high vinyl content are extremely weak compared to that between PVCH and PEP^{1,4} having very low vinyl content, and the repulsive segment−segment interactions between PVCH and PEB^{1,2} having high vinyl content are extremely weak compared to that between PVCH and PEB^{1,4} having very low vinyl content. Such experimental observations cannot be predicted using group contribution methods that cannot distinguish differences in the

Table 6. Summary of the Interaction Parameters for PS/(1,2-PB), PS/(1,4-PB), PVCH/Poly(1-Butene), and PVCH/Polyethylene Pairs Calculated Using the Group Contribution Method

Polymer pair	χ (Hoy method)
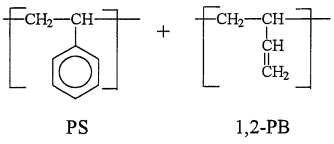 PS + 1,2-PB	0.2508 at 150 °C
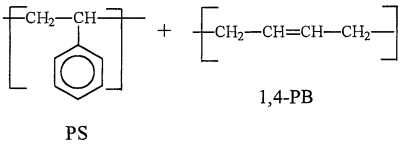 PS + 1,4-PB	0.1045 at 150 °C
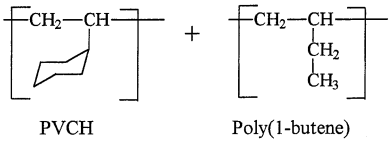 PVCH + Poly(1-butene)	0.0317 at 150 °C
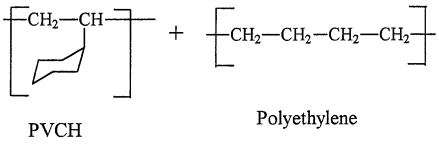 PVCH + Polyethylene	0.00608 at 25 °C 0.00318 at 50 °C 0.00043 at 100 °C 0.00005 at 150 °C

microstructures of polydienes and their saturated counterparts, as summarized in Table 6 for an illustration. Referring to Table 6, group contribution calculations[24,25] predict that the segment−segment interaction parameter χ for the PVCH/polyethylene (PE) blends is lower than that for the PS/PB[1,4] blends; thus, PVCH/PE (or PVCH/PEB[1,4]) blends are more miscible than the PS/PB[1,4] blends. If this is true, one should expect that the T_{ODT} of PVCH-*block*-PEB copolymer will be lower than that of the unsaturated precursor having a PB block with predominantly 1,4-addition, which is at variance with the experimental results reported in the literature.[9,10] On the other hand, our cloud point measurements clearly indicate that PVCH/PEB[1,4] blends are *less* miscible than the PS/PB[1,4] blends, indicating that the T_{ODT} of PVCH-*block*-PEB copolymer would be higher than that of the unsaturated precursor having a PB block with predominantly 1,4-addition, which is in agreement with experimental results.[9,10] It is worth investigating in the future the molecular origin(s) of the miscibility of PVCH/PEB[1,4], PVCH/PEB[1,2], PVCH/PEP[1,4], and PVCH/PEP[3,4] blends as affected by the microstructures of polydienes.

Acknowledgment. The authors acknowledge Matt Larive for his assistance with the hydrogenation chemistry and Daniel Murray for performing GPC analysis on the hydrogenated polymer samples.

References and Notes

(1) Ghijsels, A.; Raadsen, J. *Pure Appl. Chem.* **1980**, *52*, 1359.
(2) (a) Han, C. D.; Baek, D. M.; Kim, J. K.; Chu, S. G. *Polymer* **1992**, *33*, 294. (b) Han, J. H.; Fen, D.; Choi-Fen, C.; Han, C. D. *Polymer* **1995**, *36*, 155.
(3) Chun, S. B.; Han, C. D. *Macromolecules* **1999**, *32*, 4030.
(4) Helfand, E.; Wasserman, Z. R. In *Developments in Block Copolymers;* Goodman, I., Ed.; Applied Science: New York, 1982; Chapter 4.
(5) Leibler, L. *Macromolecules* **1980**, *13*, 1602.
(6) Hashimoto, T. In *Thermoplastic Elastomers*, 2nd ed.; Holden, G., Legge, N. R., Quirk, R., Schroeder, H. E., Eds.; Hanser: Munich, 1996; Chapter 15A and references therein.
(7) Han, C. D.; Baek, D. M.; Kim, J. K.; Ogawa, T.; Sakamoto, N.; Hashimoto, T. *Macromolecules* **1995**, *28*, 5043 and references therein.
(8) Gehlsen, M. D.; Bates, F. S. *Macromolecules* **1993**, *26*, 4122.
(9) Gehlsen, M. D.; Bates, F. S. *Macromolecules* **1994**, *27*, 3611.
(10) Adams, J. L.; Quiram, D. J.; Graessley, W. W.; Register, R. A.; Marchand, G. R. *Macromolecules* **1998**, *31*, 201.
(11) Lai, C.; Russel, W. B.; Register, R. A.; Marchand, G. R.; Adamson, D. H. *Macromolecules* **2000**, *33*, 3461.
(12) Balsara, N. P.; Lin, C. C.; Dai, H. J.; Krishnamoorti, R. *Macromolecules* **1994**, *27*, 1216.
(13) Zhao, J.; Hahn, S. F.; Hucul, D. A.; Meunier, D. M. *Macromolecules* **2001**, *34*, 1737.
(14) Han, C. D.; Chun, S. B.; Hahn, S. F.; Harper, S. Q.; Savickas, P. J.; Meunier, D. M.; Li, L.; Yalcin, T. *Macromolecules* **1998**, *31*, 394.
(15) Hucul, D. A.; Hahn, S. F. *Adv. Mater.* **2000**, *12*, 1855.
(16) Ness, J. S.; Brodil, J. C.; Bates, F. S.; Hahn, S. F.; Hucul, D. A.; Hillmyer, M. A. *Macromolecules* **2002**, *35*, 602.
(17) Roe, R.-J.; Zin, W.-C. *Macromolecules* **1980**, *13*, 1221.
(18) Richardson, M. J.; Savill, N. G. *Polymer* **1977**, *18*, 3.
(19) A Gnomix PVT apparatus was used to obtain an expression for the temperature dependence of specific volume for PVCH. The experimental procedures employed are as follows. The cell was filled with 1 g of polymer sample and 90 g of mercury; the apparatus was calibrated at 30 °C and 1 atm. Then the sample was pressurized to 10 MPa for the first run. The temperature was controlled to within ±0.1 °C, and at least 1 h after 20 °C jump was allowed for the sample to equilibrate. At a predetermined temperature data were collected at pressures of 10, 15, 20, 25, 30, 35, 40, 45, 50, 60, 70, 80, 90, and 100 MPa. For each pressure chosen, the sample is held for 40 s before data are taken. The PVT apparatus measures the volume changes in a sample between the measurement condition (temperature T and pressure P) and the reference condition (reference temperature T_r of 30 °C and reference pressure P_r of 10 MPa). The actual volume of the sample at the measurement temperature and pressure, $\tilde{V}_T^P$, was obtained by adding the volume at the reference temperature and pressure, $\tilde{V}_{30°C}^{10MPa}$, to the volume change recorded during experiment, $\Delta\tilde{V}_T^P$. The temperature dependence of specific volume above the clearing temperature of PVCH was curve-fitted to a linear relationship, $v_{PVCH} = 1.0084 + 0.6541 \times 10^{-4}(T - 273)$ (cm^3/g).
(20) Dudowicz, J.; Freed, K. F. *Macromolecules* **1991**, *24*, 5096.
(21) Dudowicz, J.; Freed, K. F. *Macromolecules* **1991**, *24*, 5112.
(22) Freed, K. F.; Dudowicz, J. *J. Chem. Phys.* **1992**, *97*, 2105.
(23) Dudowicz, J.; Freed, K. F. *Macromolecules* **1993**, *26*, 213.
(24) Billmyer, F. W. *Textbook of Polymer Science*, 3rd ed.; John Wiley: New York, 1984; Chapter 7.
(25) Sperling, L. H. *Introduction to Physical Polymer Science*, 2nd ed.; John Wiley: New York, 1993; Chapter 4.

MA0208178